Gazi Üniversitesi
Fen Bilimleri Dergisi
PART C: TASARIM VE TEKNOLOJİ

Gazi University
Journal of Science
PART C: DESIGN AND TECHNOLOGY

GU J Sci, Part C, 14(X): XX-XX (2026)

Formation Process of Cubic-Shaped Magnetite Nanoparticles by Thermal Decomposition Method and Their Surface Modification

Yeliz AKPINAR[1,2*], N. Tülün GÜRAY[3], Mürvet VOLKAN[2]

[1]*Kırşehir Ahi Evran University, Faculty of Arts and Science, Department of Chemistry, Kırşehir, Turkey*

[2]*Middle East Technical University, Faculty of Arts and Sciences, Department of Chemistry, Ankara, Turkey*

[3]*Middle East Technical University, Faculty of Arts and Sciences, Department of Biological Sciences, Ankara, Turkey*

Article Info

Research article
Received: 23/02/2026
Revision: 22/03/2026
Accepted: 22/04/2026

Keywords

Magnetic Nanoparticle, Thermal Decomposition, Nanotechnology

Makale Bilgisi

Araştırma makalesi
Başvuru: 23/02/2026
Düzeltme: 22/03/2026
Kabul: 22/04/2026

Anahtar Kelimeler

Manyetik Nanoparçacık, Termal Bozunma Metodu, Nanoteknoloji

Graphical/Tabular Abstract (Grafik Özet)

Using the thermal decomposition method, cubic-shaped magnetite nanoparticles were produced through our research efforts./ Termal bozunma metodu kullanılarak, optimizasyon çalışmları ile küp şeklilli magnitite nanoparçaık üretildi.

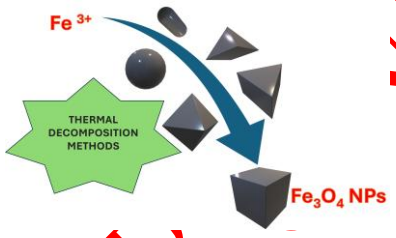

Figure A: *Thermal deposition method from iron ions to cubıc shaped Fe_3O_4 nanoparticles. /*
Şekil A: *Demir iyonlarından kübik şekilli Fe_3O_4 nanopartiküllerine termal çökelme yöntemi*

Highlights (Önemli noktalar)

- *Magnetite nanoparticles with a small size and narrow size distribution were produced for biomedical applications./ Biyomedikal kullanım amacıyla, küçük boyutta, dar boyutta dağılımına sahip manyetit nanoparçacıklar üretildi.*
- *The thermal decomposition method was used./ Termal bozunma metodu kullanıldı.*
- *Through optimization and characterization studies, the shape, crystal structure, and surface functional groups of magnetic nanoparticles were characterized../ Optimizasyon karakterizasyon çalışmları ile manyetik nanoparçacıkların şekil, kristal yapı ve yüzey fonksiyonel yapıları karaterize edildi.*

Aim (Amaç): *The aim of this study is to prepare hydrophilic cubic Fe_3O_4 NPs. / Bu çalışmanın amacı hidrofilik küp şeklinde Fe_3O_4 NPs hazırlamaktır.*

Originality (Özgünlük): *In this study, systematic optimization studies were conducted during the preparation of cubic magnetite nanoparticles, and the positive and negative results were presented along with their causes. / Bu çalışmada, küp şeklindeki manyetit nanoparçacıkların hazırlanması sırasında sistematik optimizasyon çalışmaları uygulanmış, ve olumlu/olumsuz sonuçlar sebepleriyle sunulmuştur.*

Results (Bulgular): *In the characterization studies, VSM, XRD, TEM, and FTIR spectrophotometry techniques were used. It was shown that magnetic nanoparticles modified with a hydrophilic polymer and having a cube-shaped Fe_3O_4 crystal structure with dimensions of 9.6 ± 1.2 nm were obtained. / Karakterizasyon çalışmlarında VSM, XRD, TEM ve FTIR Spektrofotometri teknikleri kullanıldı. of 9.6 ± 1.2 nm boyutuna sahio küp şekilli Fe_3O_4 kristal yapısına sahip, yüzeyi hidrofilik polimer ile modive edilmiş manyetik nanoparçacıkları elde edildiği gösterildi.*

Conclusion (Sonuç): *Magnetic nanoparticles have been prepared for use in future studies of magnetic hyperthermia therapy applications. / Gelecek çalışmalar manyetik hipertermi tedavisi uygulamalarında kullanılmak üzere manyetik nanoparçacık hazırlanmıştır.*

*Corresponding author, e-mail: yeliz.akpinar@hotmail.com
DOI: 10.29109/gujsc.1894903

GU J Sci, Part C, 14(X): XX-XX (2026)

Gazi Üniversitesi
Fen Bilimleri Dergisi
PART C: TASARIM VE TEKNOLOJİ

Gazi University
Journal of Science
PART C: DESIGN AND TECHNOLOGY

http://dergipark.gov.tr/gujsc

Formation Process of Cubic-Shaped Magnetite Nanoparticles by Thermal Decomposition Method and Their Surface Modification

Yeliz AKPINAR[1,2*], N. Tülün GÜRAY[3], Mürvet VOLKAN[2]

[1]*Kırşehir Ahi Evran University, Faculty of Arts and Sciences, Department of Chemistry, Kırşehir, Turkey*

[2]*Middle East Technical University, Faculty of Arts and Sciences, Department of Chemistry, Ankara, Turkey*

[3]*Middle East Technical University, Faculty of Arts and Sciences, Department of Biological Sciences, Ankara, Turkey*

Article Info

Research article
Received: 23/02/2026
Revision: 22/03/2026
Accepted: 22/04/2026

Keywords

Magnetic Nanoparticle, Thermal Decomposition, Nanotechnology

Abstract

The concept of nanotechnology, which first emerged in the scientific community approximately 50 years ago, continues to evolve and grow in impact without losing popularity. The extraordinary properties of materials at the nanoscale enhance human well-being across many fields, including healthcare, energy, data storage, and biomedicine. Nanoparticles are a key component of these application areas. Magnetic nanoparticles, in particular, are widely used in cancer treatment methods such as magnetic targeting and magnetic hyperthermia due to their unique magnetic properties. The shape, size, and surface modification of magnetic nanoparticles are among the critical parameters in applications aimed at cancer treatment. In this study, cubic-shaped magnetite (Fe_3O_4) nanoparticles with a size of 9.6 ± 1.2 nm and a homogeneous size distribution were synthesized using the thermal decomposition method, which is the most suitable for controlling size and shape in nanoparticle synthesis. The surfaces of the prepared cubic Fe_3O_4 nanoparticles were coated with biocompatible PVP (polyvinylpyrrolidone) to impart hydrophilic properties for use in biomedical applications. In this study, the effects of various experimental parameters (surfactant type, reaction temperature, reaction time, etc.) on the shape and size formation of magnetite nanoparticles were systematically investigated within the same study. The nanoparticles prepared during and after the optimization process were characterized using TEM, VSM, FTIR spectroscopy, and XRD.

Termal Bozunma Yöntemiyle Küp Şeklindeki Manyetit Nanopartiküllerin Oluşum Süreci ve Yüzey Modifikasyonu

Makale Bilgisi

Araştırma makalesi
Başvuru: 23/02/2026
Düzeltme: 22/03/2026
Kabul: 22/04/2026

Anahtar Kelimeler

Manyetit Nanoparçacık, Termal Bozunma Metodu, Nanoteknoloji

Öz

Yaklaşık elli yıl önce bilim dünyasında yer almaya başlayan nanoteknoloji kavramı, popülerliğini kaybetmeden etkisini artırarak gelişimini sürdürmektedir. Nano ölçekteki malzemelerin sergilediği olağanüstü özellikler, sağlık, enerji, veri depolama ve biyomedikal gibi birçok alanda insan yaşamının refahını artırmaya katkı sağlamaktadır. Bu uygulama alanlarının önemli bileşenlerinden biri de nanoparçacıklardır. Özellikle manyetik nanoparçacıklar, sahip oldukları benzersiz manyetik özellikler sayesinde kanser tedavisinde manyetik hedefleme ve manyetik hipertermi gibi yöntemlerde yaygın biçimde kullanılmaktadır. Manyetik nanoparçacıkların şekil, boyut ve yüzey modifikasyonu kanser tedavisine yönelik uygulamalarda kritik öneme sahip parametreler arasında yer almaktadır. Bu çalışmada, nanoparçacık sentezinde boyut ve şekil kontrolü için en uygun olan termal bozunma yöntemi kullanılarak homojen boyut dağılımına sahip küp şekilli 9.6±1.2 nm boyutlarında manyetit (Fe_3O_4) nanoparçacıklar sentezlenmiştir. Hazırlanan küp şeklindeki Fe_3O_4 nanoparçacıkların biyomedikal uygulamalarda kullanılmak üzere yüzeyleri biyouyumlu PVP (polivinilpirolidon) ile kaplanarak hidrofilik özellik kazandırılmıştır. Bu çalışmada farklı deneysel parametrelerin (yüzey aktif madde türü, reaksiyon sıcaklığı, reaksiyon süresi vb.) manyetit nanoparçacıklarının şekil ve boyut oluşumu üzerindeki etkileri aynı çalışma kapsamında sistematik olarak incelenmiştir. Optimizasyon sürecinde ve sonrasında hazırlanan nanoparçacıklar TEM, VSM, FTIR Spektrofotometri, ve XRD kullanılarak karakterize edildi.

*Corresponding author, e-mail: yeliz.akpinar@hotmail.com
DOI: 10.29109/gujsc.1894903

1. INTRODUCTION (GİRİŞ)

Nanotechnology is an innovative approach that enables the creation and study of materials at the molecular level. In far too many domains, including energy, ecology, health, and electronics, this method has revealed the secrets of nature. One reason for the emergence and rise of nanotechnology is the improvement in people's quality of life and longevity brought about by nanodevices, nanocomposite materials, and related technologies[1]. Nanotechnology is fundamentally based on nanoparticles. Nanoparticles are tiny pieces that are less than 100 nm in size and may consist of organic substances, metals, metal oxides, or carbon[2]. In contrast to their larger counterparts, nanoparticles exhibit unique biological, chemical, and physical characteristics [3]. Magnetic nanoparticles are widely utilized in data storage and medicinal applications. The elevated surface-to-volume ratio renders magnetic nanoparticles more appealing and advantageous compared to bulk magnetic materials [4]. Magnetic nanoparticles can be categorized into magnetic metallic nanoparticles (Co, Fe), magnetic alloy nanoparticles (Fe–Co, Fe–Ni, Fe–Pt, Co–Pt, Co–Ni), and metal oxide nanoparticles (Fe_3O_4, γ-Fe_2O_3, $NiFe_2O_4$, $MnFe_2O_4$, $CoFe_2O_4$, NiO, Co_3O_4) based on their structural composition [5], [6].

Metallic magnetic nanoparticles offer superior advantages in terms of information storage, production, and magnetic properties compared to metal oxide magnetic nanoparticles. Conversely, their chemical stability and biocompatibility are inferior to those of metal oxide nanoparticles. The elevated reactivity for oxidation and pyrophoricity of metallic magnetic nanoparticles at ambient temperature renders them unsuitable for hyperthermia applications. Despite the mitigation of oxidation through the integration of many metals with iron in the fabrication of metallic alloy magnetic nanoparticles, metal oxide nanoparticles remain the favored choice for biomedical applications [7], [8], [9], [10].

There are eight types of iron oxides; however, maghemite (γ-Fe_2O_3), hematite (α-Fe_2O_3), and magnetite (Fe_3O_4) are the most recognized. The crystalline structure of iron oxide nanoparticles influences their applicability, particularly in fields such as medicine, electronics, and environmental remediation. Magnetic characteristics vary according to crystal structures. They are sought after for technological and biomedical applications due to their distinctive magnetic, biochemical, and catalytic capabilities [11].

In this study, magnetite (Fe_3O4) nanoparticles have been focused on. Magnetite is referred to as black iron oxide. Its magnetic saturation exceeds that of the other two types of iron oxide nanoparticles due to a lower oxygen ratio compared to maghemite (γ-Fe_2O_3) and hematite (α-Fe_2O_3). Maghemite can be readily synthesized through the oxidation of magnetite [12]. Magnetite possesses an inverse spinel crystal structure, characterized by a polyhedral model with stacking arrangements. The face-centered cubic (fcc) unit cell includes $32O^{2-}$ ions, which are systematically arranged in a cubic-close-packed configuration along the [111] plane. Electrons can transition between Fe^{2+} and Fe^{3+} ions at the octahedral sites at ambient temperature, establishing magnetite as a crucial grouping of half-metallic materials [11], [12]. Magnetite can be synthesized using various methods. Co-precipitation [13], electrochemical methods [14], sol-gel methods [15], solvothermal/hydrothermal methods [16], laser ablation [17], ball milling [18], and thermal decomposition methods [19], etc.

The thermal decomposition method is commonly used to produce superparamagnetic magnetite nanoparticles. This technique relies on the high-temperature breakdown of organic precursors of iron in the presence of organic solvents and surfactants. The type of surfactant, decomposition temperature, reflux duration, and solvent influence the control of shape and size [19]. The advantages of thermal decomposition methods include, first, that the crystallinity of iron oxide nanoparticles is superior to that of those manufactured via co-precipitation methods. High crystallinity is achieved at elevated temperatures. The second advantage is that iron oxide nanoparticles exhibit a restricted size distribution. Additionally, surfactants confer monodispersity in solution, resulting in minimal aggregation. The third advantage is that the regulation of size and shape is more manageable with thermal decomposition procedures [19], [20].

Optimization is essential for the production of iron oxide nanoparticles, encompassing multiple parameters, including iron precursors, temperature, solvent, surfactant types, reaction duration, and heating rate. Typical iron precursors contain $Fe(CO)_5$, iron oleate, and ferrocene, all of which demonstrate low solubility in water [21]. Dewi et al. indicated that modifying the heating rate and reaction duration can affect the morphology of the particles, shifting from spherical to cubic and enlarging their dimensions by 5-10 nm in their study [22]. The selection of solvent is crucial, as thermal degradation generally requires elevated temperatures (exceeding 250°C), attainable with organic solvents with high boiling points, such as

octadecene and benzyl ether, which subsequently influence particle size. Surfactants such as oleic acid and sodium oleate are crucial in regulating the morphology and dimensions of nanoparticles. The study by Sun et al. showed that spherical iron oxide nanoparticles are produced using oleylamine as a surfactant and benzyl ether as a solvent, with decomposition occurring at 298 °C [23]. In contrast, Dewi et al. demonstrated that cubic-shaped iron oxide nanoparticles may be synthesized using sodium oleate as a surfactant and octadecene as a solvent [22].

The literature indicates that cubic magnetic nanoparticles are preferable for biomedical applications, particularly for cancer treatment. Specific Absorption Rate (SAR) values have been measured to be higher in cubic magnetite nanoparticles compared to spherical ones, suggesting they may yield more effective results in magnetic hyperthermia therapy [24]. Furthermore, their planar surface indicates that cubic particles have more effective surface functions in surface-to-surface interactions. Therefore, they offer advantages in drug delivery and targeting studies [25].

The primary disadvantage of this approach is the acquisition of hydrophobic nanoparticles. Aqueous media are essential for numerous applications, particularly in the biomedical field. The generation of hydrophobic iron oxide nanoparticles constitutes the primary drawback of this approach for biological applications. By implementing ligand exchange and coating techniques, these particles become hydrophilic[26]. Polyvinylpyrrolidone [27], poly(maleic anhydride-alt-1-octadecene)[28], and 3,4-dihydroxyhydrocinnamic acid [29] may serve as examples of ligand exchange and coating agents.

The preparation of magnetite nanocube nanoparticles is available in the literature. The thermal decomposition method was first reported by Sun et al. The nanoparticles they prepared had a spherical, uniform shape [30]. Marzan et al. and Kim et al. demonstrated that the size and shape control of magnetic nanoparticles can be modified through optimization studies using the same method [31], [32]. Kim et al. optimized the reflux time[33], while Muro-Cruces et al. demonstrated the effect of the iron precursor amount on the shape[34]. Saengruengrit et al., on the other hand, have developed methods for preparing nanocubes of different sizes by varying both the reflux time and the reaction temperature[35]. Ulrich et al. demonstrated the effects of surfactant and heating rate on magnetite shape in their study [36], [37]. For approximately 20 years, unique procedures have been developed and reported by optimizing parameters using the same methodology.

This study aimed to obtain cube-shaped, monodisperse magnetite nanoparticles with homogeneous shape and size via thermal decomposition methods. This study was initiated by referencing the work of Kim et al.[33]. The particles they prepared were approximately 70 nm in size. To obtain smaller, more uniform nanoparticles, the method was modified in the same study by changing the precursor, surfactant, initial heating time, complex formation time, reflux time, co-surfactant, and procedure, and a unique procedure was developed, with each step reported and illustrated with TEM images. Also, this study has demonstrated the negative outcomes/reasons for the systematic application of known procedures, as well as the positive effects of optimization studies. Finally, since the produced magnetite nanoparticles will be used for biomedical purposes in future studies, they were made hydrophilic using the PVP coating method.

2.MATERIALS AND METHODS (MATERYAL VE METOD)

In this study, the thermal decomposition method was applied to obtain cubic-shaped magnetite nanoparticles. The graphical summary of methods is given in Figure 1.

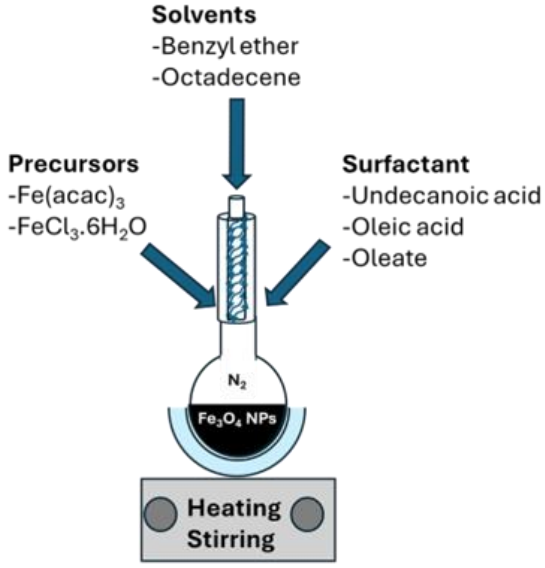

Figure 1. Graphical summary of applied thermal decomposition method (Uygulanan termal bozunma yönteminin grafiksel özeti)

Materials

Iron(III)acetylacetonate ($Fe(acac)_3$, (≥97%)), Ferric chloride hexahydrate ($FeCl_3 \cdot 6H_2O$ (≥97%)), Oleic acid (≥97%), benzyl ether (97%), Undecanoic acid((98%) Sodium oleate (≥82%), Polyvinylpyrolidone (average mol wt 10,000), N, N-Dimethylformamide, (99.8%), Hexane (≥97%), Toluene (≥98% anhydrous) were purchased from SIGMA-ALDRICH. Acetone (for analysis), Chloroform (ACS, ISO, Reag. Ph Eur.), Ethanol (absolute suitable for use as an excipient) Dichloromethane (LiChrosolv®) were supplied by MERCK. Octadecene was used with ≥95% grade, FLUKA.

2.1. Synthesis of Cubic Iron Oxide Nanoparticles Utilizing Undecanoic Acid and Oleic Acid as Surfactants (Yüzey aktif madde olarak undekanoik asit ve oleik asit kullanılarak kübik demir oksit nanopartiküllerinin sentezi)

The thermal decomposition approach was employed to manufacture cubic-shaped Fe3O4 nanoparticles. 0.5 mmol of $Fe(acac)_3$, 2 mmol of oleic acid, and 12.5 mL of benzyl ether were subjected to degassing for 1 hour at 60 °C under a nitrogen environment in a three-necked round-bottom flask. The temperature was subsequently elevated to 200 °C at a rate of 4 °C per minute. The mixture was agitated at this temperature for approximately 2.5 hours, after which the temperature was elevated to the reflux point (298 °C) at a heating rate of 2 °C/min. After 1 hour of stirring at reflux temperature, the black precipitate was washed with a mixture of acetone and ethanol, then dispersed in chloroform. Table 1, A [33]. All reactions were carried out in an air-free medium under N_2 gas.

Undecanoic acid substituted oleic acid in the previously mentioned thermal degradation procedure. The times for the complex formation, initial heating, and refluxing heating periods were optimized under these settings, as shown in Table 1 (B, C, D, E, F, G).

Table 1. Optimization parameters of the thermal decomposition technique by using oleic acid and undecanoic acid as a surfactant (Oleik asit ve undekanoik asidin yüzey aktif madde olarak kullanıldığı termal bozunma tekniğinin optimizasyon parametreleri)

Experiment Name	Complex Formation Heating Time	Initial Heating Time (Hour)	Reflux Time (Minute)	Amount of Acid (mmol)
A	60	2.5	60	2.0
B	60	2.5	60	2.0
C	45	2.5	60	2.0
D	45	2.5	45	2.0
E	45	1.0	45	2.0
F	45	1.5	45	2.0
G	45	1.5	45	1.5

2.2. Synthesis of Cubic-Shaped Iron Oxides by Using Oleic Acid–Sodium Oleate as a Surfactant (Oleik Asit–Sodyum Oleatın Yüzey Aktif Madde Olarak Kullanılmasıyla Kübik Şekilli Demir Oksitlerin Sentezi)

A novel approach was implemented to elevate the reflux temperature, utilizing a mixture of oleic acid and sodium oleate as a surfactant. Iron oleate was produced by combining 3 mmol sodium oleate, 15.0 mL water, 8.95 g oleic acid, 10 mmol $FeCl_3 \cdot 6H_2O$, 20.0 mL ethanol, and 35.0 mL hexane for 4 hours at 70°C. Following washing the product with water and hexane, a brown paste was obtained, identified as iron oleate. In the thermal decomposition technique, 0.95 g of iron oleate was dissolved in 0.16 g of octadecene and agitated for 1 hour at 200 °C, after which the temperature was elevated to the reflux temperature of approximately 310 °C. After one hour of stirring at this temperature, a washing technique was implemented, and the nanoparticles were dispersed in hexane (Table 2, A) [22] N_2 gas was used as an inert medium.

Table 2. Optimization studies of the synthesis of cubic-shaped iron oxides by using oleic acid-sodium oleate as a surfactant (Oleik asit-sodyum oleat karışımını yüzey aktif madde olarak kullanarak kübik şekilli demir oksitlerin sentezinin optimizasyon çalışmaları)

Experiment Name	Iron–oleate complex formation in the reaction medium	NaCl Addition
A	No	No
B	Yes	No
C	Yes	Yes

The approach proposed by Xu et al. was also used to synthesize cubic iron oxide nanoparticles. The iron oleate complex was not synthesized independently in this approach. All precursors (0.25 mmol $FeCl_3 \cdot 6H_2O$, 1.5 mmol sodium oleate, and 5.0 mL octadecene) were agitated for 1 hour at 130 °C. The mixture was thereafter agitated for 2 hours and 20 minutes at a reflux temperature of approximately 317 °C. After cooling to the outside temperature, the magnetic nanoparticles were washed using an ethanol, water, and hexane mixture via extraction and subsequently dispersed in toluene (Table 2, B). The approach proposed by Xu et al. was subsequently modified. The iron oleate complex was synthesized using the initial approach. Sodium oleate was utilized as the surfactant in the thermal decomposition technique. 0.25 mmol of iron oleate, 0.75 mmol of sodium oleate, 0.75 mmol of sodium chloride, and 5.0 mL of octadecene were stirred continuously for 1 hour at 130°C. The temperature was subsequently increased to the

reflux temperature of approximately 317 °C, and the mixture was stirred for 2 hours and 20 minutes at that temperature. The particles were then washed using the same extraction procedure as in the previous trial and dispersed in toluene (Table 2, C) [33], [38].

2.3. Modification of Iron Oxide Nanoparticles from Hydrophobic to Hydrophilic State (Demir Oksit Nanoparçacıklarının Hidrofobik Halden Hidrofilik Hale Dönüştürülmesi)

To create hydrophilic iron oxide nanoparticles that are cube-shaped. The hydrophobic cube-shaped magnetic nanoparticles were placed in a volume of 0.6 mL, and a 5.0 mL DMF/DCM (1/1) mixture and 60 mg of polyvinylpyrrolidone (PVP) were added under agitation. The last mixture of ingredients was incubated for 10 hours at 100 °C. The white precipitate formed when 10 mL of diethyl ether was added to the mixture dropwise. Ethanol was used to wash the precipitate, which was then dispersed in water[39] .

3. RESULTS (BULGULAR)

The thermal decomposition method was employed to synthesize cubic-shaped Fe3O4 nanoparticles. The production of Fe-oleate complexes and elevated reflux temperatures (exceeding 300 °C) are crucial for the synthesis of cubic-shaped iron oxide nanoparticles.

The literature reports that in thermal decomposition methods, initial heating, reflux time, and surfactant type affect particle shape and morphology [40], [41]. Kim et al. reported that they obtained nanocups with sharper corners when they increased the reflux time [33]. Additionally, Wang et al. reported that they obtained magnetic nanoparticles with various shapes by using different chains and saturation numbers with an amine group as a surfactant[42]. In this study, with this approach, attempts were made to obtain cube-shaped magnetite nanoparticles step by step using various surfactants and different reflux-intermediate heating times (Table 1 and Table 2). The results of the optimization studies applied in the experimental part are given below.

3.1. Synthesis of Cubic Iron Oxide Nanoparticles Utilizing Undecanoic Acid and Oleic Acid as Surfactants (Undekanoik Asit ve Oleik Asit Yüzey Aktif Maddeleri Kullanılarak Kübik Demir Oksit Nanoparçacıklarının Sentezi)

Oleic acid acted as a surfactant and stabilizer. The primary difference among the approaches employed to synthesize spherical magnetite was the separation of the heating stage into three parts: complex formation duration, initial heating, and reflux period. Degassed precursors were agitated for 1 hour at 60 °C under a nitrogen atmosphere, after which the temperature was raised to 200 °C, and agitation continued for 2.5 hours (Table 1, A). The

Fe-oleate complex was anticipated to form during the heating phase at 60 °C. A one-hour high-temperature reflux was utilized for the breakdown of the resultant complex in the creation of cubic iron oxide nanoparticles. The maximum temperature attainable under this scenario was 290 °C.

Transmission electron microscopy (TEM) was used to characterize the particles' morphology. The TEM image and the size histogram, derived from nanoparticle measurements, are presented in Figure 2. The nanoparticles exhibited a size range of 5–8 nm and were strongly monodisperse. Nevertheless, their forms predominantly resemble triangular prisms. Only a limited number of cubic buildings were observed.

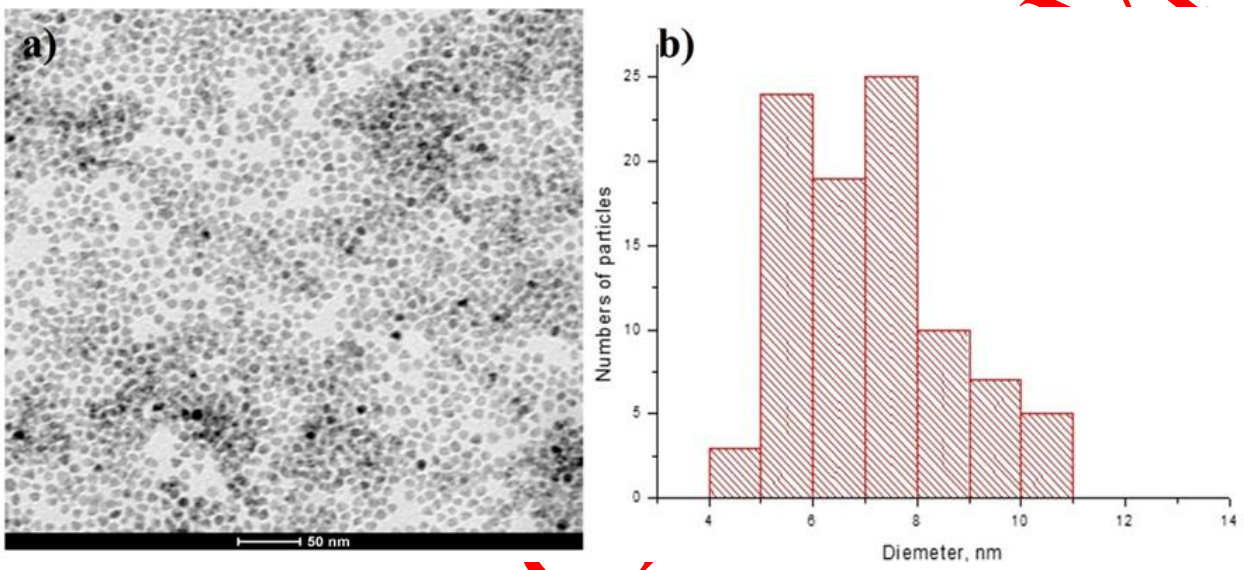

Figure 2. TEM picture and size histogram of nanoparticles synthesized using thermal decomposition methods utilizing oleic acid as a surfactant (Table 1,A)) (Oleik asidin yüzey aktif madde olarak kullanıldığı termal bozunma yöntemleriyle sentezlenen nanopartiküllerin TEM görüntüsü ve boyut histogramı (Tablo 1, A))

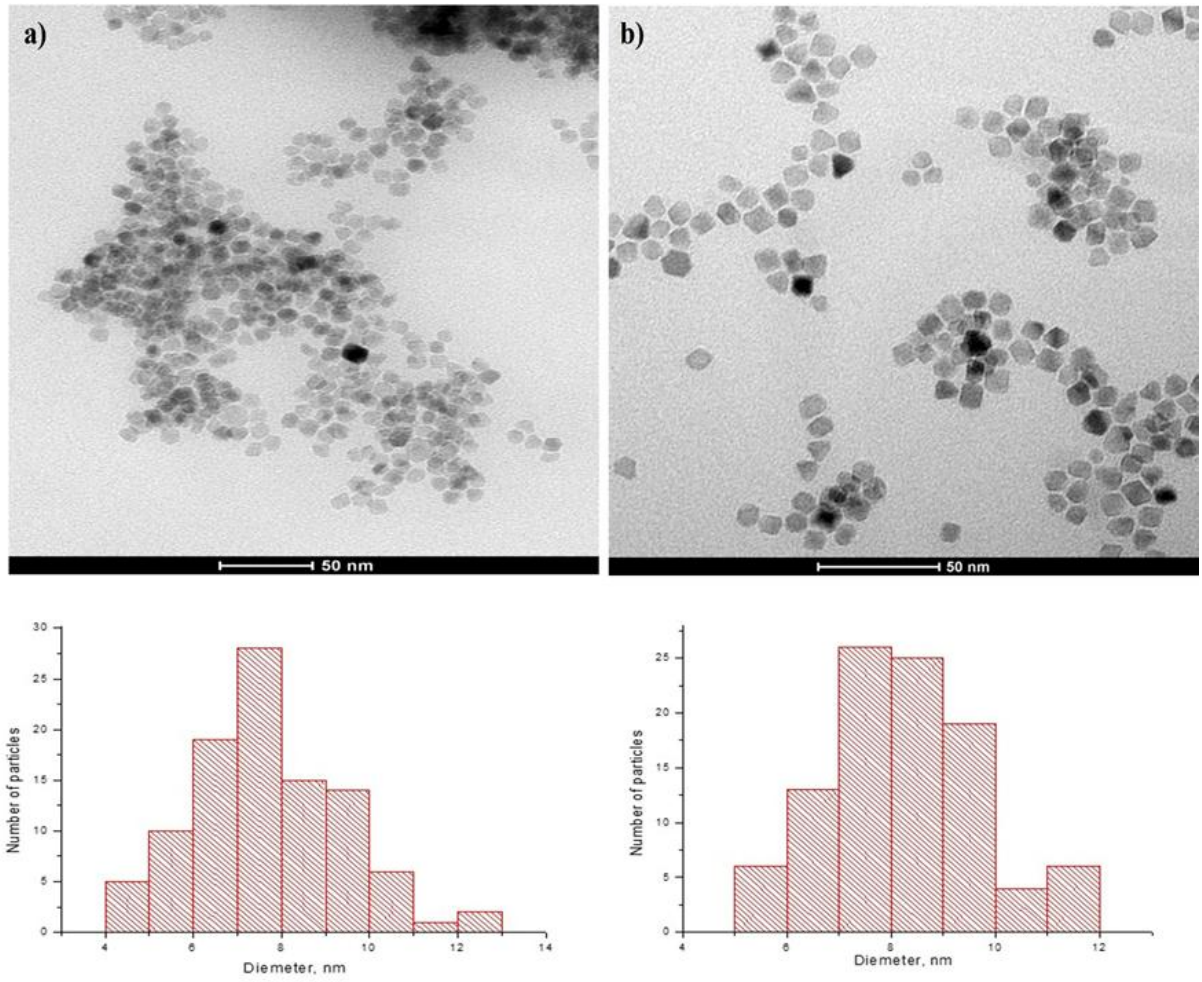

Figure 3. TEM pictures of iron oxide nanoparticles produced in undecanoic acid using a) 1 h heating time (Table 1, B), and b) 45 minute heating period for complex synthesis (Table 1, C). The corresponding nanoparticle size distribution histograms are provided beneath each TEM image (Undekanoik asit kullanılarak a) 1 saat ısıtma süresi (Tablo 1, B), ve b) kompleks sentez için 45 dakika ısıtma süresi (Tablo 1, C) ile üretilen demir oksit nanopartiküllerinin TEM görüntüleri. Her TEM görüntüsünün altında ilgili nanopartikül boyut dağılımı histogramları verilmiştir)

Subsequently, the surfactant was altered. Undecanoic acid was utilized in place of oleic acid. Oleic acid comprises eighteen carbon atoms with a double bond between the ninth and tenth carbon, resulting in an angular conformation, whereas undecanoic acid includes a ten-carbon methyl chain. The impact of complex formation duration on shape controls was initially evaluated. A complex formation period of 1 h and 45 minutes was conducted at 60 °C. Both studies had an initial heating period of 2.5 hours at 200 °C, followed by a 1-hour reflux at the maximum temperature. Transmission electron microscopy pictures are presented in Figure 3.

A reduction in the period of complex formation yields a greater quantity of cubic-shaped particles. Consequently, a complex formation time of 45 minutes was chosen, and the intermediate heating time was adjusted to 1.0-2.5 hours. Figure 4 presents TEM pictures of the particles. Based on TEM images, no notable differences in size or form were detected.

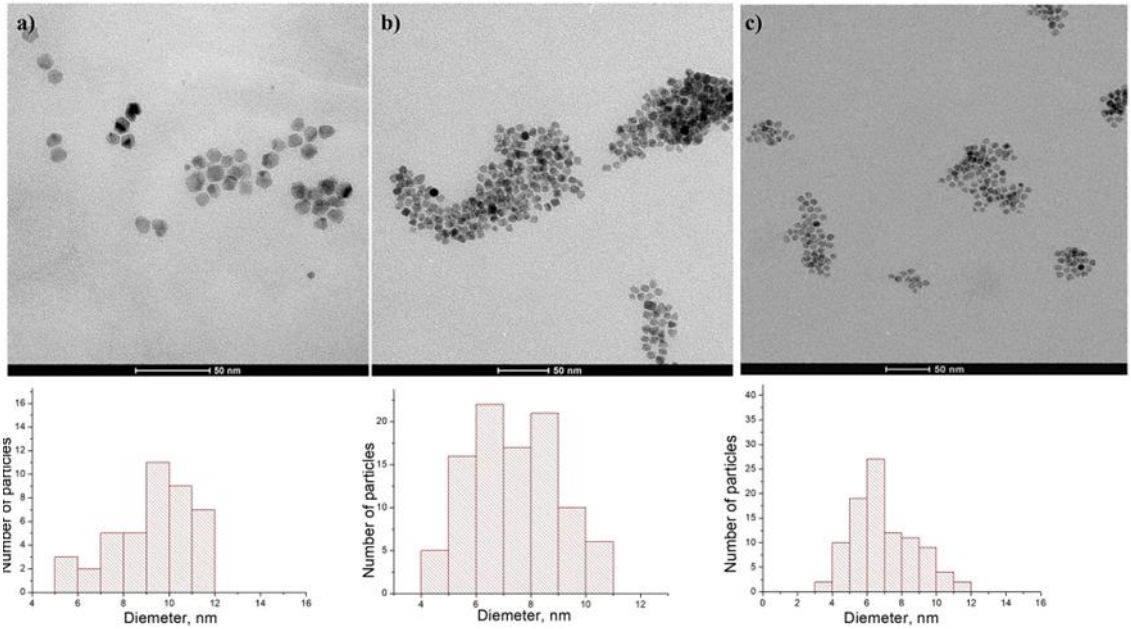

Figure 4. TEM pictures of magnetite nanoparticles synthesized in undecanoic acid with a) 2.5 hours(Table 1, D), b) 1 hour(Table 1, E), and c) 1.5 hours (Table 1, F) of intermediate heating at a constant complex formation temperature of 60 °C for 45 minutes, followed by a reflux duration of 45 minutes. The size distribution histograms of the nanoparticle are presented below each TEM image (Undekanoik asit içinde sentezlenen manyetit nanopartiküllerinin TEM görüntüleri; sırasıyla a) 2,5 saat(Tablo 1, D) , b) 1 saat(Tablo 1, E) ve c) 1,5 saat (Tablo 1, F) süreyle, 60°C'lik sabit kompleks oluşum sıcaklığında 45 dakika süreyle ara ısıtma ve ardından 45 dakika süreyle geri akış işlemi uygulandıktan sonra elde edilmiştir. Nanopartikülün boyut dağılım histogramları her TEM görüntüsünün altında sunulmuştur)

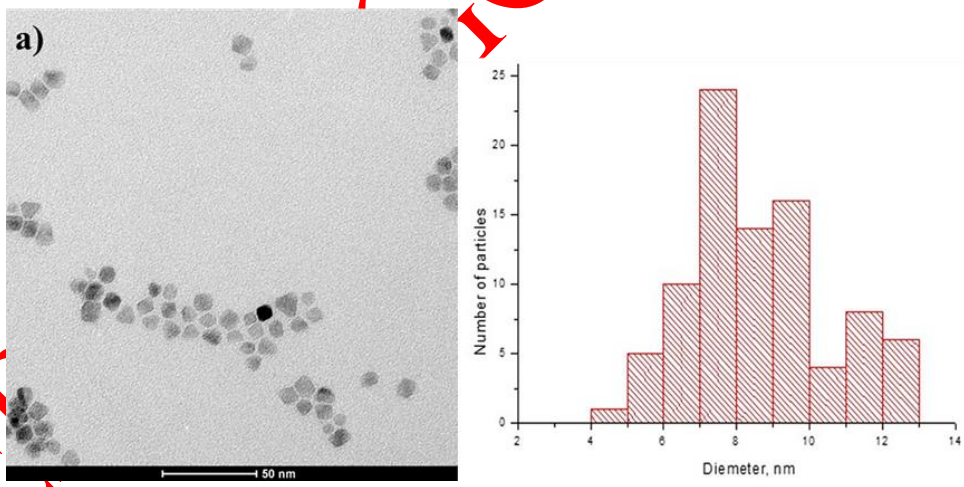

Figure 5. TEM images of iron oxide nanoparticles synthesized with a reduced concentration of undecanoic acid (one-quarter of the original amount), a 45-minute complex formation period at 60 °C, 1.5 hours of intermediate heating at 200 °C, and 45 minutes of refluxing at the maximum achievable temperature(Table 1, G). The histogram depicting the size distribution of the nanoparticles is presented below the TEM image (Azaltılmış konsantrasyonda undekanoik asit (orijinal miktarın dörtte biri) kullanılarak sentezlenen demir oksit nanopartiküllerinin TEM görüntüleri; 60 °C'de 45 dakikalık kompleks oluşum süresi, 200 °C'de 1,5 saatlik ara ısıtma ve ulaşılabilir maksimum sıcaklıkta 45 dakikalık geri akış işlemi uygulanmıştır(Tablo 1, G). Nanopartiküllerin boyut dağılımını gösteren histogram, TEM görüntüsünün altında sunulmuştur)

The impact of surfactant quantity was assessed during a 45 minutes complex formation period at 60 °C, followed by 1.5 hours of intermediate heating at 200 °C, and a 45-minute reflux at the maximum achievable temperature. Figure 5 shows the TEM image and its associated size distribution histogram

After reducing the undecanoic acid content by one-fourth, as illustrated in Figure 5, cubic-shaped magnetite nanoparticles were produced; however, the morphology and size distribution were not uniform. Throughout these trials, the main difficulty was to keep the temperature above 300 °C and maintain stability during refluxing. At times, it reached 298 °C, then decreased by approximately 20 °C. The boiling point of benzyl ether is 298 °C. It was supposed that the boiling point of the benzyl ether solution comprising the reaction precursors and surfactants (oleic or undecanoic acid) would exceed that of the pure compound. Benzyl ether is found to degrade at temperatures over 310-350 °C. The order and rate of this disintegration process are influenced by acid, glass surfaces, and contaminants [43], [44] The reduction in temperature is likely attributable to the breakdown of benzyl ether at temperatures below 300 °C, influenced by the presence of oleic or undecanoic acid and other potential contaminants in the reaction media. Temperature appears to play a paramount role in regulating particle morphology. To address this problem, a change in solvent and surfactant was decided on.

.

3.2. Synthesis of Cubic-Shaped Iron Oxides by Using Oleic Acid–Sodium Oleate as a Surfactant

(Oleik Asit-Sodyum Oleatın Yüzey Aktif Madde Olarak Kullanılmasıyla Kübik Şekilli Demir Oksitlerin Sentezi)

Three evaluations were conducted utilizing sodium oleate and oleic acid as surfactants. In all experiments, 1-octadecane served as the solvent, allowing the reflux temperature to exceed 310 °C

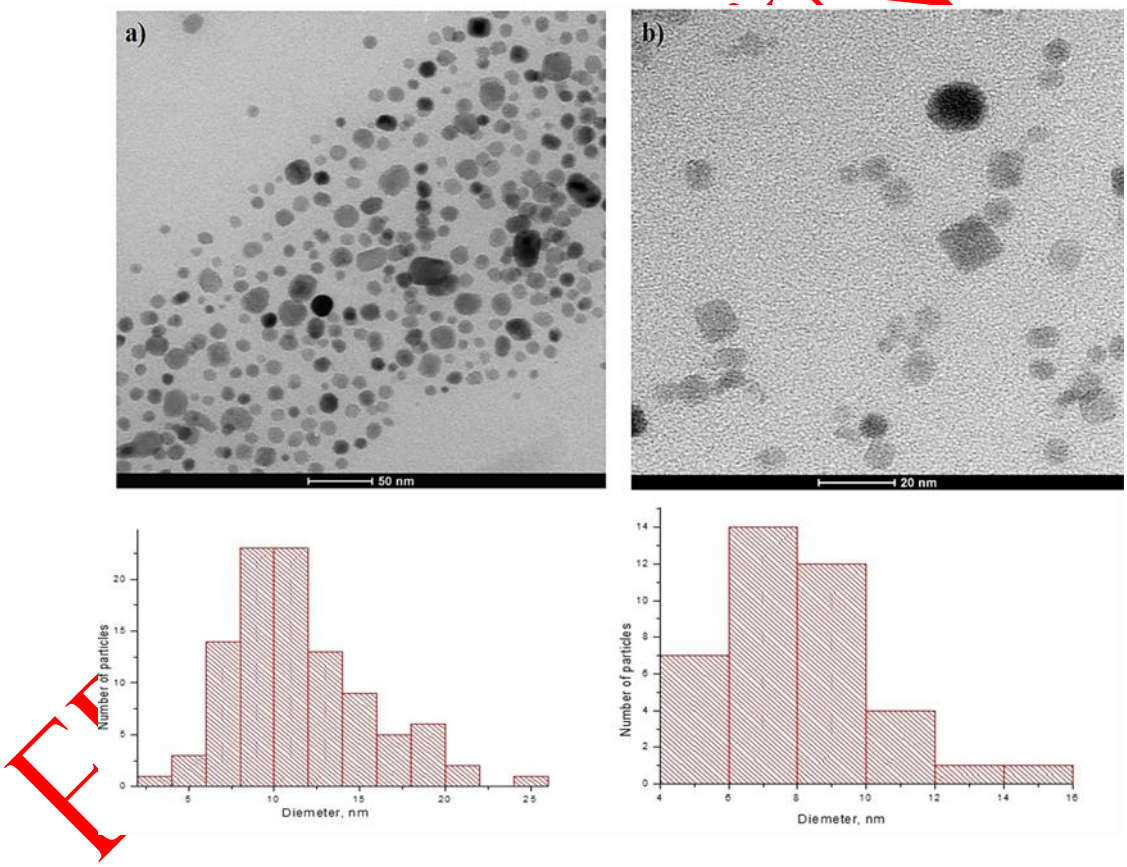

Figure 6. TEM pictures of iron oxide nanoparticles manufactured utilizing a) Fe-oleate-oleic acid (Table 2,A), and b) sodium oleate (without the preparation of the Fe-oleate complex) (Table 2,B) as the surfactant system ((a) Fe-oleat-oleik asit (Tablo 2,A) ve b) sodyum oleat (Fe-oleat kompleksi hazırlanmadan) (Tablo 2,B) yüzey aktif madde sistemi kullanılarak üretilen demir oksit nanopartiküllerinin TEM görüntüleri)

Initially, the Fe-oleate combination was synthesized independently and subsequently combined with oleic acid. The TEM image in Figure 6a indicates that the size distribution is suboptimal, with the majority of particles exhibiting a spherical morphology (Table 2,A).

In the second experiment, the process of Fe-oleate complex formation was eliminated; the precursor and surfactants were combined simultaneously. Upon examining the TEM picture in Figure 6b, it is evident that while predominantly cubic forms were generated, spherical particles were also present. Furthermore, there exists significant variability in their dimensions (5 - 25 nm) (Table 2,B).

In the third experiment (Table 2,C), identical experimental circumstances were utilized as in the preceding experiment. The sole distinction was the application of sodium chloride. Xu et al. indicated that halogen ions significantly contribute to the creation of cubic-shaped metal oxide nanoparticles, especially chlorides[38].

Figure 7 shows a TEM picture of cubic-shaped iron oxide nanoparticles. The TEM image indicates that all iron oxide nanoparticles have a cubic morphology, with a narrow size distribution ranging from 8 to 11 nm and an average size of 9.6 ± 1.2 nm. This observation demonstrates the influence of Cl^- on the development of cubic-shaped particles.

NaCl is not merely a byproduct in the creation of the intermediate; it is also a crucial chemical for the morphological regulation of iron oxide nanocrystals. Xu et al. asserted that Cl ions may efficiently stabilize the {100} facets of cubic spinel-structured iron oxide nanocrystals and promote the development of cubic-shaped nanocrystals. The role of Cl ions likely arises from the minimal atomic packing density in the {100} planes of cubic spinel, where only Fe atoms are densely arranged, facilitating the effective coordination of Cl ions with Fe atoms. In the absence of Cl, the utilization of $Fe(acac)_3$ as a precursor resulted in the formation of non-cubic shaped nanocrystals with a broad size distribution[38].

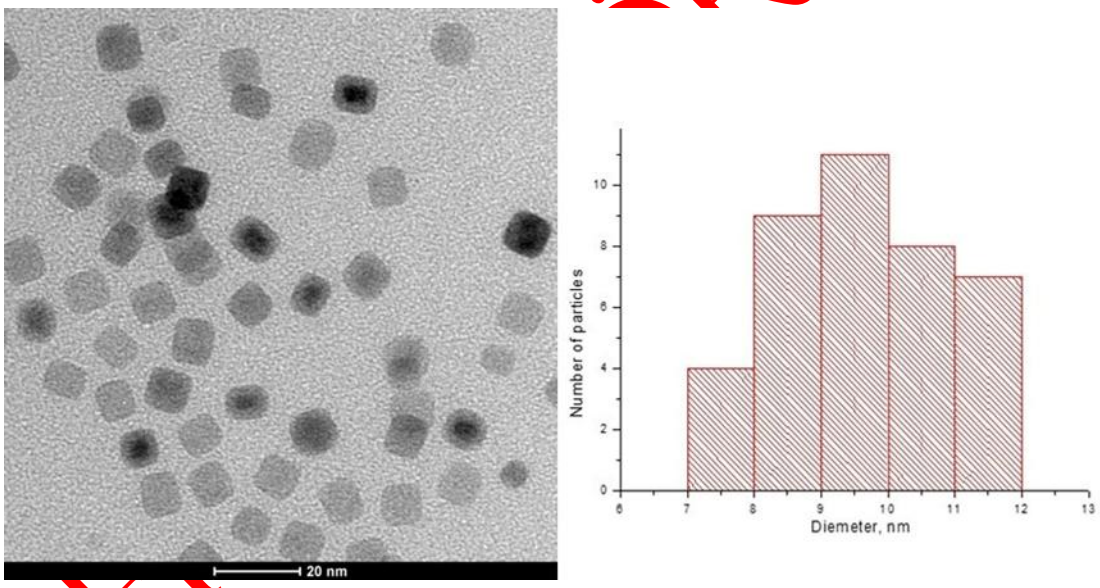

Figure 7. TEM images of sodium oleate and sodium chloride-synthesised cubic iron oxide nanoparticles. The nanoparticles' corresponding size distribution histogram is displayed next to the TEM picture (Table 2,C) (Sodyum oleat ve sodyum klorür ile sentezlenen kübik demir oksit nanopartiküllerinin TEM görüntüleri. Nanopartiküllerin karşılık gelen boyut dağılım histogramı TEM resminin yanında gösterilmiştir (Tablo 2, C))

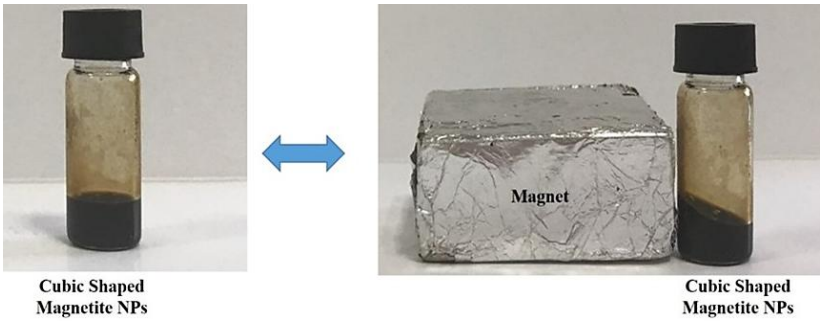

Figure 8. The behaviors of nanoparticles of iron oxide with a cubic form in nearby to the magnet (Kübik formdaki demir oksit nanopartiküllerinin mıknatısa yakın ortamdaki davranışları)

Figure 8 illustrates how the cubic-shaped nanoparticles behave when exposed to a magnetic field. Although they were not entirely collected, they were collected on the magnet's side 60 seconds after being placed close to it.

X-ray diffraction (XRD) was employed for structural characterisation. The baseline-corrected XRD pattern has been included in the original XRD pattern of cubic-shaped iron oxide nanoparticles, as shown in Figure 9. The distinctive peak of magnetite iron oxide is depicted in the XRD pattern (Figure 9). The analysis was conducted within the angular range of $10^{o} \leq 2\theta \leq 90^{o}$, revealing Bragg reflections for (2 2 0), (3 3 1), (4 0 0), (4 2 2), (5 1 1), and (4 4 0) at 2θ values of 30.13°, 35.81°, 43.16°, 53.48°, 57.25°, 62.72°, and 73.88°, respectively, which correspond to the characteristic 2θ values of magnetite (JCPDS No: 19-0629) [45], [46].

.

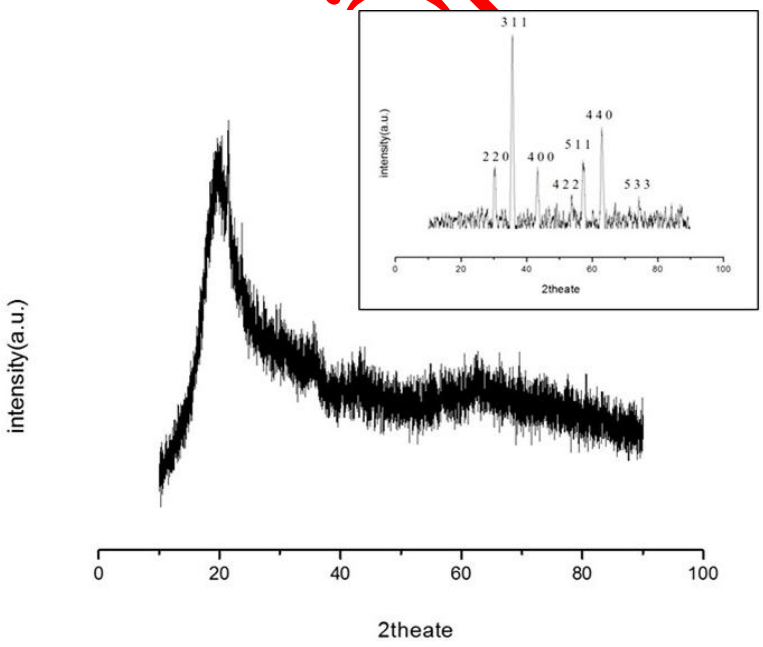

Figure 9. X-ray diffraction pattern of cubic iron oxide nanoparticles. The baseline-corrected spectrum has been implemented into the graph (Kübik demir oksit nanopartiküllerinin X-ışını kırınım deseni. Temel çizgi düzeltmesi yapılmış spektrum grafiğe dahil edilmiştir)

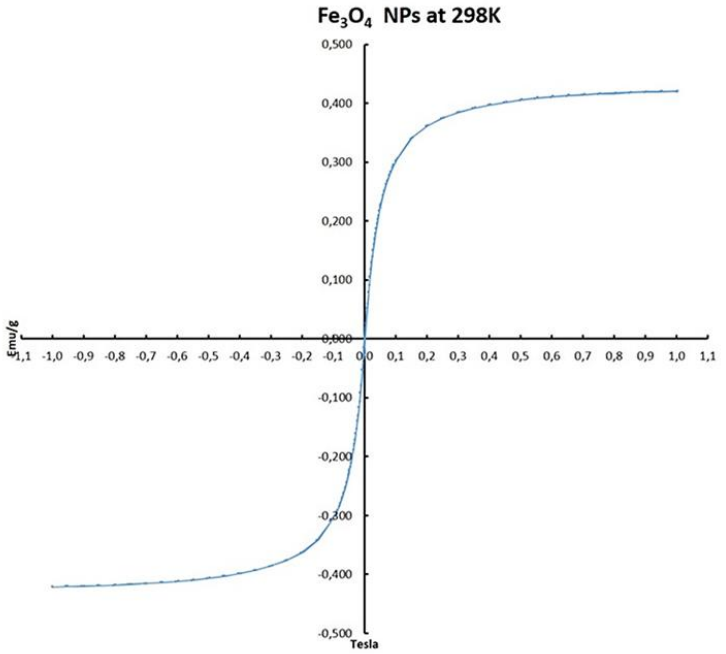

Figure 10. Magnetization and magnetic field curves for cubic-shaped iron oxide nanoparticles (Table 2,C) at 298 K (Kübik şekilli demir oksit nanopartiküllerinin 298 K'deki manyetizasyon ve manyetik alan eğrileri (Tablo 2, C))

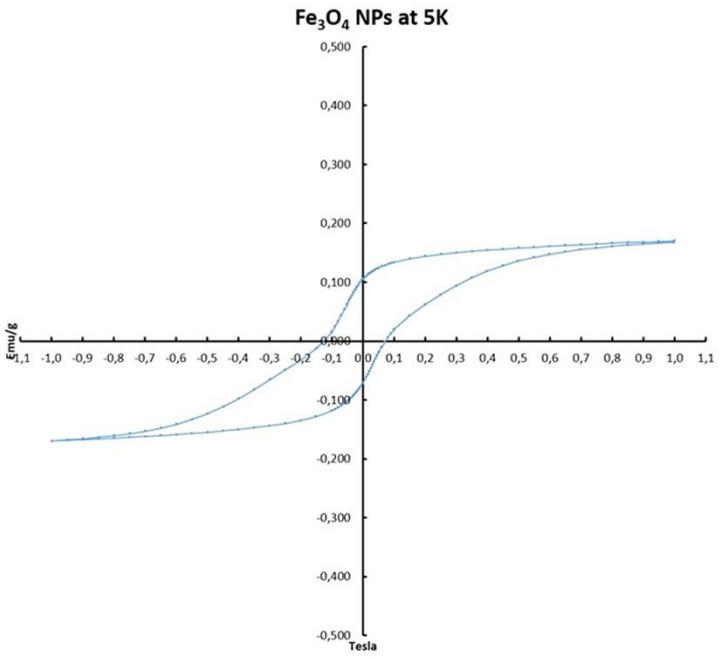

Figure 11. Magnetization and magnetic field curves for cubic-shaped iron oxide nanoparticles (Table 2,C) at 270 K (Kübik şekilli demir oksit nanopartiküllerinin 5 K'deki manyetizasyon ve manyetik alan eğrileri (Tablo 2, C))

Magnetization measurements were conducted using a field scan from ±1.1 T at 298 K and 5 K. The magnetization vs magnetic field curves of cubic-shaped iron oxide nanoparticles (Table 2, C) were generated at these two temperatures. Figure 10 illustrates the magnetic properties of cubic-shaped iron oxide nanoparticles assessed at 298 K.

The Ms values of our cubic-shaped iron oxide nanoparticles were compared to the published values. Typically, the magnetic saturation value for magnetite iron oxide nanoparticles measuring 10-20 nm exceeds 1 emu/g [47], [48]. Superparamagnetic behavior was discovered in cubic-shaped iron oxide nanoparticles at 298 K, as illustrated in Figure 10. As illustrated in the figure, they exhibit zero coercivity in the absence of a magnetic field. Nevertheless, the Ms value was too low, approximately 0.4 emu/g.

Figure 11illustrates the magnetization (Ms) as a function of the applied magnetic field (H) for cubic iron oxide nanoparticles. Table 2, C, at 5 K, below the Tb of cubic-shaped magnetite nanoparticles (about 270 K) [43]. As anticipated, our nanocubes exhibit hysteresis at 5K. Figure 11 illustrates that the saturation magnetization (Ms) of the nanocubes is 0.12 emu/g, while their remanent magnetization (Mr) is 0.1 emu/g. In fact, the measurement should exceed 1 emu/g. The results were unsatisfactory due to sampling issues and device sensitivity. The magnetic data suggest the synthesis of superparamagnetic cubic-shaped magnetite nanoparticles.

This inadequate outcome was likely associated with the challenges encountered during the sample preparation phase. Due to the presence of a considerable amount of surfactants, cubic-shaped iron oxide nanoparticles were unable to be dried correctly, and liquid remained in the form of adhesive jelly. The VSM measurement was conducted using a powder sample rather than a liquid sample. This physical hardship may have adversely impacted the measurements. Helendra et al. reported in their study that non-magnetic coatings, such as oleate, reduce the Ms value of magnetite nanoparticles. They claim that oleic acid coating surrounds magnetite nanoparticles, reducing the volume of active magnetic material and leading to a decrease in magnetic moment density despite a constant number of particles. This layer can disrupt the spin order of the nanoparticles, leading to spin disorder that diminishes the overall contribution of surface magnetic moments. The oleic acid also alters the dipolar interactions, diminishing magnetic contacts between nanoparticles and resulting in decreased saturation magnetization due to the formation of a non-magnetic monolayer on their surfaces[49]. The low Ms values of the magnetite nanoparticles in gel-liquid form, which we prepared with an excessive amount of oleate-oleic acid coating, can be explained by the Helendra et al. interpretation.

In addition, Kolhatkar et al. reported that the Ms value decreases as the magnetic nanoparticle size decreases to 10 nm or smaller. This is because, as the size of magnetic nanoparticles decreases, the structure shifts from a multi-domain to a single-domain state, and supermagnetism increases. As a result, coercivity and magnetic saturation decrease[50]. Small size and high SAR are desirable properties for nanoparticles used in magnetic hyperthermia applications. While heat generation in hyperthermia applications occurs via hysteresis loss in large magnetic nanoparticles, for nanoparticles below 10 nm, it occurs via Neel relaxation. This ensures that medium density, like tissue, has no effect on heat generation. Therefore, small magnetic nanoparticles have become the preferred choice for magnetic hyperthermia applications [51], [52], [53], [54]. For this reason, we aimed to synthesize small, supermagnetic nanoparticles for magnetic hyperthermia application. As a result, to obtain an efficient SAR value for magnetic hyperthermia application, optimization studies need to be carried out on exposure time, magnetic nanoparticle concentration, magnetic field amplitude, and frequency [55].

3.3. Modification of Iron Oxide Nanoparticles from Hydrophobic to Hydrophilic State (Demir Oksit Nanopartiküllerinin Hidrofobik Durumdan Hidrofilik Duruma Dönüştürülmesi)

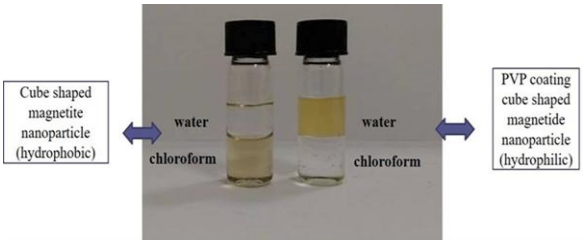

Figure 12. Photograph of cubic-shaped magnetic nanoparticles suspended in an aqueous medium following PVP coating (PVP kaplamasının ardından sulu ortamda süspansiyon halinde bulunan küp şeklindeki manyetik nanopartiküllerin fotoğrafı)

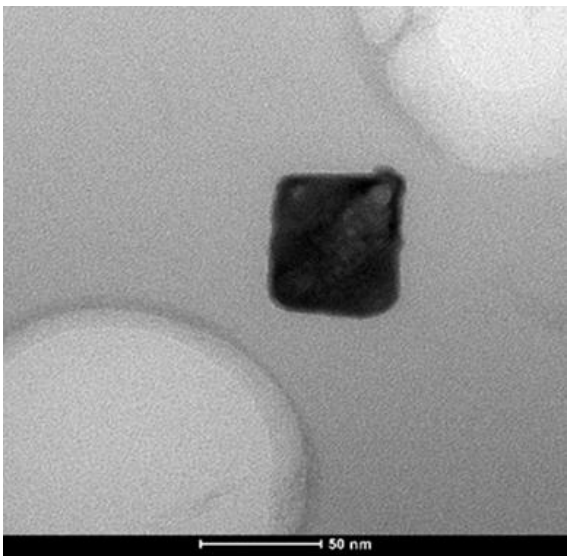

Figure 13. TEM picture of iron oxide nanoparticles covered with PVP (PVP ile kaplanmış demir oksit nanopartiküllerinin TEM görüntüsü)

The hydrophobic surfaces of Fe_3O_4 nanoparticles were altered to display hydrophilicity by including an excess of amphiphilic polyvinylpyrrolidone (PVP) to cubic-shaped magnetic nanoparticles, facilitating the exchange of the oleate ligand on the nanoparticles with PVP. After modification, Fe_3O_4 nanoparticles could be redispersed in hydrophilic solvents like ethanol and water. Figure 12 illustrates that PVP-coated iron oxide nanoparticles remain in the aqueous phase, but the hydrophobic variants, as synthesized, favor the chloroform phase. Additionally, no agglomeration of magnetic nanoparticles was observed in the aqueous phase. The change in this property proves that the oleate ligands on Fe_3O_4 nanoparticles were effectively substituted by PVP [27].

Figure 13 displays a TEM image of PVP-coated iron oxide nanoparticles. The bare, cubic-shaped iron oxide nanoparticles measure 10 nm and are coated with a 20 nm PVP coating. Their geometrical parameters remained unchanged following the coating treatment. Furthermore, no aggregation of the Fe_3O_4 nanoparticles was seen following ligand exchange.

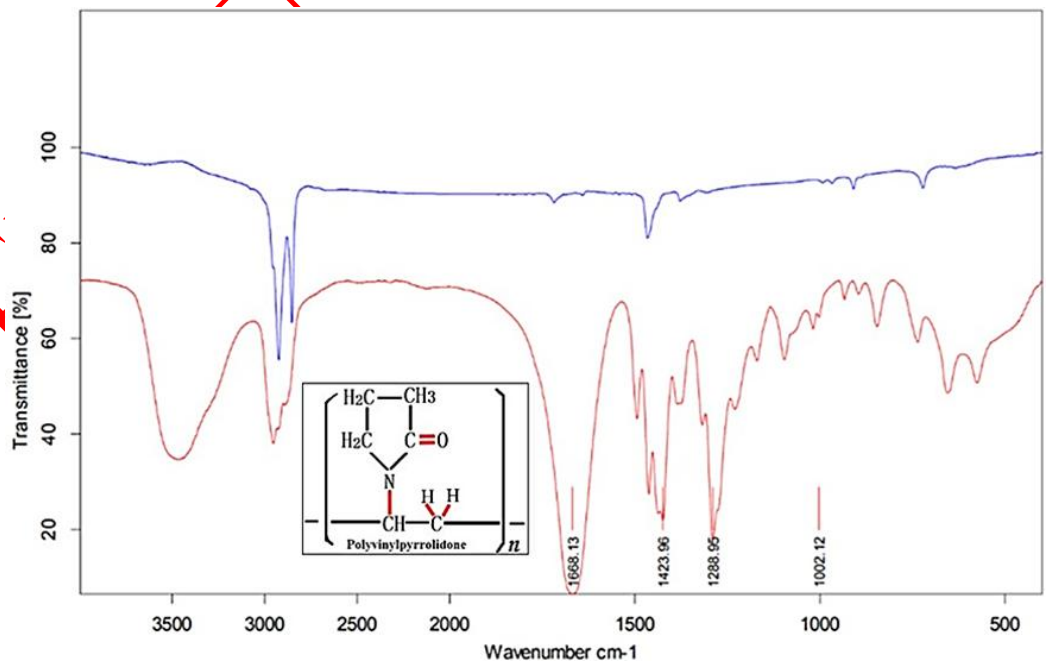

Figure 14. FTIR spectra of iron oxide nanoparticles covered with PVP (PVP ile kaplanmış demir oksit nanopartiküllerinin FTIR spektrumları)

The PVP coating process has been examined further using FTIR Spectrophotometer measurements. Figure 14 presents the IR spectra of uncoated (blue line) and PVP-coated (red line) cubic-shaped iron oxide nanoparticles. The bands at 1668.13 cm^{-1} and 1423 cm-1 correspond to C=O stretching vibrations and CH2 bending, respectively. The bands at 1288.95 cm^{-1} and 1005 cm^{-1} correspond to the typical stretching of C-N bonds. The emergence of these new peaks signifies the successful coating of cubic-shaped hydrophobic iron oxide nanoparticles with PVP [48], [56].

4. CONCLUSIONS (SONUÇLAR)

In this study, cubic magnetite nanoparticles with a narrow size distribution were prepared and modified to make their surfaces hydrophilic. Additionally, the study demonstrated and discussed the effects of various optimization parameters (surfactant, backflow time, reaction temperature, etc.) on the formation of nanoparticle geometry. Finally, due to the decomposition of the most commonly used solvent, benzyl ether, at high temperatures in the presence of oleic acid and its inability to maintain the temperature required to obtain a cubic shape, octadecene was used as the solvent, oleate as the surfactant, and NaCl as the additive, resulting in magnetite nanoparticles with homogeneous sizes of 9.6 ± 1.2 nm. The characterization results, including TEM images, XRD patterns, VSM curves, and FTIR spectra, confirm that the desired hydrophilic magnetite nanoparticles have been obtained. As a result, we have developed our inventive method.

These magnetic nanoparticles have been prepared for a cubic shape, which as had been reported in the literature with a small size and high SAR value for potential use in magnetic hyperthermia treatment in the future. However, their low Ms value, due to their size and surface coatings, indicates that these nanoparticles are not ready for use in magnetic hyperthermia. For this reason, the surface-cleaning process of the newly prepared nanoparticles will be conducted more carefully, and optimization studies will be conducted on parameters such as exposure time, magnetic nanoparticle concentration, magnetic field amplitude, and frequency to achieve a high SAR value for magnetic hyperthermia studies.

ACKNOWLEDGMENTS (TEŞEKKÜR)

This article is derived from part of the PhD thesis submitted by Yeliz AKPINAR (METU, 2017), and this study was supported by TÜBİTAK awarding grant (2211A) and ÖYP-DPT through Project BAP-08-11-DPT.2011K121010. The authors are grateful to Prof. Dr. Ayşen YILMAZ (METU, Department of Chemistry) for her support in the XRD measurements. / Bu makale, Yeliz AKPINAR tarafından (ODTÜ, 2017) sunulan doktora tezinin bir bölümünden türetilmiştir ve bu çalışma TÜBİTAK (2211A) bursu ile ÖYP-DPT tarafından BAP-08-11-DPT.2011K121010 numaralı proje aracılığıyla desteklenmiştir. Yazarlar, XRD ölçümlerindeki desteklerinden dolayı Prof. Dr. Ayşen YILMAZ'a (ODTÜ, Kimya Bölümü) teşekkür ederler.

DECLARATION OF ETHICAL STANDARDS (ETİK STANDARTLARIN BEYANI)

The author of this article declares that the materials and methods they use in their work do not require ethical committee approval and/or legal-specific permission.

Bu makalenin yazarı çalışmalarında kullandıkları materyal ve yöntemlerin etik kurul izni ve/veya yasal-özel bir izin gerektirmediğini beyan ederler.

AUTHORS' CONTRIBUTIONS (YAZARLARIN KATKILARI)

***Yeliz AKPINAR*:** She conducted the experiments, analyzed the results and performed the writing/editing process.

Deneyleri yapmış, sonuçlarını analiz etmiş ve makalenin yazım işlemini gerçekleştirmiştir.

***N. Tülün GÜRAY* :** She supervised and consultant project/study, and contributed writing/ editing process.

Proje/çalışmaların denetimini ve danışmanlığını üstlendi ve yazım/düzenleme sürecine katkıda bulundu.

***Mürvet VOLKAN*:** She supervised and consultant project/study, and contributed writing/ editing process.

Proje/çalışmaların denetimini ve danışmanlığını üstlendi ve yazım/düzenleme sürecine katkıda bulundu.

CONFLICT OF INTEREST (ÇIKAR ÇATIŞMASI)

There is no conflict of interest in this study.

Bu çalışmada herhangi bir çıkar çatışması yoktur.

REFERENCES (KAYNAKLAR)

[1] S. Malik, K. Muhammad, and Y. Waheed, "Nanotechnology: A Revolution in Modern Industry," Molecules, vol. 28, no. 2, p. 661, Jan. 2023, doi: 10.3390/molecules28020661.

[2] H. Ateş and E. Bahçeci, "Nano Malzemeler için Üretim Yöntemleri," Gazi Üniversitesi Fen Bilimleri Dergisi Part:C, Tasarım Ve Teknoloji, no. 3(2), p. 483499, 2015.

[3] Y. Khan et al., "Classification, Synthetic, and Characterization Approaches to Nanoparticles, and Their Applications in Various Fields of Nanotechnology: A Review," Catalysts, vol. 12, no. 11, p. 1386, Nov. 2022, doi: 10.3390/catal12111386.

[4] S. Singamaneni, V. N. Bliznyuk, C. Binek, and E. Y. Tsymbal, "Magnetic nanoparticles: recent advances in synthesis, self-assembly and applications," J. Mater. Chem., vol. 21, no. 42, p. 16819, 2011, doi: 10.1039/c1jm11845e.

[5] S. B. Dalavi, A. B. Patil, and R. N. Panda, "Magnetic Nanoparticles-Based Coated Materials," 2024, pp. 533–571. doi: 10.1007/978-981-97-4646-0_16.

[6] K. Chand and E. S. Vasquez-Guardado, "Magnetic Nanoparticles: Synthesis and Applications in Life Sciences," ChemistryOpen, vol. 14, no. 12, Dec. 2025, doi: 10.1002/open.202500214.

[7] Z. Hedayatnasab, F. Abnisa, and W. M. A. W. Daud, "Review on magnetic nanoparticles for magnetic nanofluid hyperthermia application," Mater. Des., vol. 123, pp. 174–196, Jun. 2017, doi: 10.1016/j.matdes.2017.03.036.

[8] Mittal, A., Roy, I., and Gandhi, S., "Magnetic Nanoparticles: An Overview for Biomedical Applications." Magnetochemistry, vol.8, no.9, pp.107.2022,doi:10.3390/magnetochemistry8090107

[9] M. D. Nguyen et al., "Magnetic Iron Oxide Nanoparticles: Advances in Synthesis, Mechanistic Understanding, and Magnetic Property Optimization for Improved Biomedical Performance," Nanomaterials, vol. 15, no. 19, p. 1500, Oct. 2025, doi: 10.3390/nano15191500.

[10] R. Ghazi et al., "Iron oxide based magnetic nanoparticles for hyperthermia, MRI and drug delivery applications: a review," RSC Adv., vol. 15, no. 15, pp. 11587–11616, 2025, doi: 10.1039/D5RA00728C.

[11] W. Wu, C. Z. Jiang, and V. A. L. Roy, "Designed synthesis and surface engineering strategies of magnetic iron oxide nanoparticles for biomedical applications," Nanoscale, vol. 8, no. 47, pp. 19421–19474, 2016, doi: 10.1039/C6NR07542H.

[12] J. Santoyo Salazar et al., "Magnetic Iron Oxide Nanoparticles in 10−40 nm Range: Composition in Terms of Magnetite/Maghemite Ratio and Effect on the Magnetic Properties," Chemistry of Materials, vol. 23, no. 6, pp. 1379–1386, Mar. 2011, doi: 10.1021/cm103188a.

[13] S. T. Aly et al., "Preparation of magnetite nanoparticles and their application in the removal of methylene blue dye from wastewater," Sci. Rep., vol. 14, no. 1, p. 20100, Aug. 2024, doi: 10.1038/s41598-024-69790-w.

[14] H. Setyawan and W. Widiyastuti, "Progress in the Preparation of Magnetite Nanoparticles through the Electrochemical Method," KONA Powder and Particle Journal, vol. 36, no. 0, p. 2019011, Jan. 2019, doi: 10.14356/kona.2019011.

[15] P. N. Brahmbhatt, S. R. Bharucha, A. Bhatt, and M. S. Dave, "The Synthesis, Characterization, and Antimicrobial Activity of Magnetite (Fe_3O_4) Nanoparticles by the Sol–Gel Method," in The 4th International Electronic Conference on Applied Sciences, Basel Switzerland: MDPI, Nov. 2023, p. 293. doi: 10.3390/ASEC2023-15950.

[16] N. Torres-Gómez, O. Nava, L. Argueta-Figueroa, R. García-Contreras, A. Baeza-Barrera, and A. R. Vilchis-Nestor, "Shape Tuning of Magnetite Nanoparticles Obtained by Hydrothermal Synthesis: Effect of Temperature," J. Nanomater., vol. 2019, pp. 1–15, Feb. 2019, doi: 10.1155/2019/7921273.

[17] N. G. Semaltianos and G. Karczewski, "Laser Synthesis of Magnetic Nanoparticles in Liquids and Application in the Fabrication of Polymer–Nanoparticle Composites," ACS Appl. Nano Mater., vol. 4, no. 7, pp. 6407–6440, Jul. 2021, doi: 10.1021/acsanm.1c00715.

[18] J. F. de Carvalho, S. N. de Medeiros, M. A. Morales, A. L. Dantas, and A. S. Carriço, "Synthesis of magnetite nanoparticles by high energy ball milling," Appl. Surf. Sci., vol. 275, pp. 84–87, Jun. 2013, doi: 10.1016/j.apsusc.2013.01.118.

[19] A. A. Demessie et al., "An Advanced Thermal Decomposition Method to Produce Magnetic Nanoparticles with Ultrahigh Heating Efficiency for Systemic Magnetic Hyperthermia," Small Methods, vol. 6, no. 12, Dec. 2022, doi: 10.1002/smtd.202200916.

[20] W. Wu, Z. Wu, T. Yu, C. Jiang, and W. S. Kim, "Recent progress on magnetic iron oxide nanoparticles: Synthesis, surface functional strategies and biomedical applications," Sci.

Technol. Adv. Mater., vol. 16, no. 2, 2015, doi: 10.1088/1468-6996/16/2/023501.

[21] W. Glasgow et al., "Continuous synthesis of iron oxide (Fe_3O_4) nanoparticles via thermal decomposition," Particuology, vol. 26, pp. 47–53, Jun. 2016, doi: 10.1016/j.partic.2015.09.011.

[22] M. R. Dewi, W. M. Skinner, and T. Nann, "Synthesis and Phase Transfer of Monodisperse Iron Oxide (Fe3O4) Nanocubes," Aust. J. Chem., vol. 67, no. 4, pp. 663–669, Apr. 2014, doi: 10.1071/CH13595.

[23] S. N. Sun, C. Wei, Z. Z. Zhu, Y. L. Hou, S. S. Venkatraman, and Z. C. Xu, "Magnetic iron oxide nanoparticles: Synthesis and surface coating techniques for biomedical applications," Chinese Physics B, vol. 23, no. 3, pp. 1–19, 2014, doi: 10.1088/1674-1056/23/3/037503.

[24] I. Astefanoaei, R. Gimaev, V. Zverev, A. Tishin, and A. Stancu, "Cubic and Sphere Magnetic Nanoparticles for Magnetic Hyperthermia Therapy: Computational Results," Nanomaterials, vol. 13, no. 16, p. 2383, Aug. 2023, doi: 10.3390/nano13162383.

[25] A. B. Jindal, "The effect of particle shape on cellular interaction and drug delivery applications of micro- and nanoparticles," Int. J. Pharm., vol. 532, no. 1, pp. 450–465, Oct. 2017, doi: 10.1016/j.ijpharm.2017.09.028.

[26] N. Zhu et al., "Surface Modification of Magnetic Iron Oxide Nanoparticles," Nanomaterials, vol. 8, no. 10, p. 810, Oct. 2018, doi: 10.3390/nano8100810.

[27] K. Kadel, S. Mirshahghassemi, and J. R. Lead, "Facile Flow-Through Synthesis Method for Production of Large Quantities of Polyvinylpyrrolidone-Coated Magnetic Iron Oxide Nanoparticles for Oil Remediation," Environ. Eng. Sci., vol. 35, no. 2, pp. 67–75, Feb. 2018, doi: 10.1089/ees.2016.0577.

[28] G. C. Lavorato et al., "Hydrophilization of magnetic nanoparticles with an amphiphilic polymer revisited: Roles of nanoparticle capping density and polymer structure," Appl. Surf. Sci., vol. 570, p. 151171, Dec. 2021, doi: 10.1016/j.apsusc.2021.151171.

[29] Y. Liu et al., "Facile Surface Functionalization of Hydrophobic Magnetic Nanoparticles," J. Am. Chem. Soc., vol. 136, no. 36, pp. 12552–12555, Sep. 2014, doi: 10.1021/ja5060324.

[30] S. Sun and H. Zeng, "Size-Controlled Synthesis of Magnetite Nanoparticles," J. Am. Chem. Soc., vol. 124, no. 28, pp. 8204–8205, Jul. 2002, doi: 10.1021/ja026501x.

[31] A. Shavel, B. Rodríguez-González, M. Spasova, M. Farle, and L. M. Liz-Marzán, "Synthesis and Characterization of Iron/Iron Oxide Core/Shell Nanocubes," Adv. Funct. Mater., vol. 17, no. 18, pp. 3870–3876, Dec. 2007, doi: 10.1002/adfm.200700494.

[32] D. Kim, J. Park, K. An, N.-K. Yang, J.-G. Park, and T. Hyeon, "Synthesis of Hollow Iron Nanoframes," J. Am. Chem. Soc., vol. 129, no. 18, pp. 5812–5813, May 2007, doi: 10.1021/ja070667m.

[33] D. Kim, N. Lee, M. Park, B. H. Kim, K. An, and T. Hyeon, "Synthesis of uniform ferrimagnetic magnetite nanocubes," J. Am. Chem. Soc., vol. 131, no. 2, pp. 454–455, 2009, doi: 10.1021/ja8086906.

[34] J. Muro-Cruces et al., "Precise Size Control of the Growth of Fe_3O_4 Nanocubes over a Wide Size Range Using a Rationally Designed One-Pot Synthesis," ACS Nano, vol. 13, no. 7, pp. 7716–7728, Jul. 2019, doi: 10.1021/acsnano.9b01281.

[35] C. Saengruengrit et al., "Iron oxide nanospheres and nanocubes modified with carboxyphenyl porphyrin and their magnetic, optical properties and photocatalytic activities in room temperature amide synthesis," J. Magn. Magn. Mater., vol. 521, p. 167515, Mar. 2021, doi: 10.1016/j.jmmm.2020.167515.

[36] A. Ullrich, M. M. Rahman, A. Azhar, M. Kühn, and M. Albrecht, "Synthesis of iron oxide nanoparticles by decomposition of iron-oleate: influence of the heating rate on the particle size," Journal of Nanoparticle Research, vol. 24, no. 9, p. 183, Sep. 2022, doi: 10.1007/s11051-022-05554-9.

[37] J. Park et al., "Ultra-large-scale syntheses of monodisperse nanocrystals," Nat. Mater., vol. 3, no. 12, pp. 891–895, Dec. 2004, doi: 10.1038/nmat1251.

[38] Z. Xu, C. Shen, Y. Tian, X. Shi, and H.-J. Gao, "Organic phase synthesis of monodisperse iron oxide nanocrystals using iron chloride as precursor," Nanoscale, vol. 2, no. 6, p. 1027, 2010, doi: 10.1039/b9nr00400a.

[39] W. Y. Rho et al., "Facile synthesis of monodispersed silica-coated magnetic nanoparticles," Journal of Industrial and Engineering Chemistry, vol. 20, no. 5, pp. 2646–2649, 2014, doi: 10.1016/j.jiec.2013.12.014.

[40] A. Lu, E. L. Salabas, and F. Schüth, "Magnetic Nanoparticles: Synthesis, Protection, Functionalization, and Application," Angew. Chem. Int. Ed., vol. 46, no. 8, pp. 1222–1244, Feb. 2007, doi: 10.1002/anie.200602866.

[41] Y. Eom, M. Abbas, H. Noh, and C. Kim, "Morphology-controlled synthesis of highly crystalline Fe_3O_4 and $CoFe_2O$ nanoparticles using a facile thermal decomposition method," RSC Adv., vol. 6, no. 19, pp. 15861–15867, 2016, doi: 10.1039/C5RA27649G.

[42] D. Wang, P. Yang, and Y. Zhu, "Growth of Fe_3O_4 nanoparticles with tunable sizes and morphologies using organic amine," Mater. Res. Bull., vol. 49, pp. 514–520, Jan. 2014, doi: 10.1016/j.materresbull.2013.09.019.

[43] P. Guardia et al., "One pot synthesis of monodisperse water soluble iron oxide nanocrystals with high values of the specific absorption rate," J. Mater. Chem. B, vol. 2, no. 28, p. 4426, 2014, doi: 10.1039/c4tb00061g.

[44] K. E. Gilbert and J. J. Gajewski, "Coal liquefaction model studies: free radical chain decomposition of diphenylpropane, dibenzyl ether, and phenethyl phenyl ether via .beta.-scission reactions," J. Org. Chem., vol. 47, no. 25, pp. 4899–4902, Dec. 1982, doi: 10.1021/jo00146a016.

[45] Y. Li, Z. Wang, and R. Liu, "Superparamagnetic α-Fe_2O_3/Fe_3O_4 Heterogeneous Nanoparticles with Enhanced Biocompatibility," Nanomaterials, vol. 11, no. 4, p. 834, Mar. 2021, doi: 10.3390/nano11040834.

[46] W. LU, M. LING, M. JIA, P. HUANG, C. LI, and B. YAN, "Facile synthesis and characterization of polyethylenimine-coated Fe3O4 superparamagnetic nanoparticles for cancer cell separation," Mol. Med. Rep., vol. 9, no. 3, pp. 1080–1084, Mar. 2014, doi: 10.3892/mmr.2014.1906.

[47] J. Muro-Cruces et al., "Precise Size Control of the Growth of Fe_3O_4 Nanocubes over a Wide Size Range Using a Rationally Designed One-Pot Synthesis," ACS Nano, vol. 13, no. 7, pp. 7716–7728, Jul. 2019, doi: 10.1021/acsnano.9b01281.

[48] M. R. Dewi, W. M. Skinner, and T. Nann, "Synthesis and phase transfer of monodisperse iron oxide (Fe_3O_4) nanocubes," Aust. J. Chem., vol. 67, no. 4, pp. 663–669, 2014, doi: 10.1071/CH13595.

[49] Helendra, N. I. Istiqomah, H. Sabarman, and E. Suharyadi, "Synthesis of varied oleic acid-coated Fe_3O_4 nanoparticles using the co-precipitation technique for biosensor applications," Sensors International, vol. 6, p. 100295, 2025, doi: 10.1016/j.sintl.2024.100295.

[50] A. Kolhatkar, A. Jamison, D. Litvinov, R. Willson, and T. Lee, "Tuning the Magnetic Properties of Nanoparticles," Int. J. Mol. Sci., vol. 14, no. 8, pp. 15977–16009, Jul. 2013, doi: 10.3390/ijms140815977.

[51] M. Ma, Y. Wu, J. Zhou, Y. Sun, Y. Zhang, and N. Gu, "Size dependence of specific power absorption of Fe_3O_4 particles in AC magnetic field," J. Magn. Magn. Mater., vol. 268, no. 1–2, pp. 33–39, Jan. 2004, doi: 10.1016/S0304-8853(03)00426-8.

[52] V. Narayanaswamy et al., "Role of Magnetite Nanoparticles Size and Concentration on Hyperthermia under Various Field Frequencies and Strengths," Molecules, vol. 26, no. 4, p. 796, Feb. 2021, doi: 10.3390/molecules26040796.

[53] H. Gavilán et al., "How size, shape and assembly of magnetic nanoparticles give rise to different hyperthermia scenarios," Nanoscale, vol. 13, no. 37, pp. 15631–15646, 2021, doi: 10.1039/D1NR03484G.

[54] C. Iacovita et al., "Small versus Large Iron Oxide Magnetic Nanoparticles: Hyperthermia and Cell Uptake Properties," Molecules, vol. 21, no. 10, p. 1357, Oct. 2016, doi: 10.3390/molecules21101357.

[55] B. Kozissnik, A. C. Bohorquez, J. Dobson, and C. Rinaldi, "Magnetic fluid hyperthermia: Advances, challenges, and opportunity," International Journal of Hyperthermia, vol. 29, no. 8, pp. 706–714, Dec. 2013, doi: 10.3109/02656736.2013.837200.

[56] M. Karegar and M. M. Khodaei, "Synthesis of Fe_3O_4-PVP nanocomposite functionalized with sulfonic group as an effective catalyst for one-pot synthesis of xanthene derivatives," Research on Chemical Intermediates, vol. 47, no. 11, pp. 4537–4555, Nov. 2021, doi: 10.1007/s11164-021-04542-3.